# Magnetism and thermodynamics of defect-free Fe-Cr alloys

T. P. C. Klaver,[1,*] R. Drautz,[2] and M. W. Finnis[1,†]
[1]*School of Mathematics and Physics, Queen's University Belfast, Belfast BT7 1NN, Northern Ireland, United Kingdom*
[2]*Department of Materials, University of Oxford, Parks Road, Oxford OX1 3PH, United Kingdom*
(Received 23 January 2006; revised manuscript received 7 July 2006; published 29 September 2006)

Density functional theory calculations have been used to study the mixing behavior of Fe-Cr alloys. The heats of formation $\Delta E_f$ of 65 Fe-Cr structures in their magnetic ground states have been determined. A positive $\Delta E_f$ is found over most of the concentration range. From 0–12 % Cr a small negative $\Delta E_f$ down to −8 meV/atom is found. The origin of the negative $\Delta E_f$ in Fe-rich structures is traced to the solution energy of single Cr atoms. At low concentration, Cr atoms in Fe repel each other, causing ordering. The Cr-Cr interactions are well reproduced even without the self-consistent relaxation of the electron density and the positions of atoms. Multi-ion (or concentration-dependent) interactions are indispensable in order to describe the whole phase diagram. The interesting magnetic situation that arises when ferromagnetic and antiferromagnetic metals are mixed in different ratios is discussed with reference to nearest- and next-nearest-neighbor clusters of Cr in Fe. Magnetic frustration leads to a strong dependence of the Cr moment on the number of Cr neighbors. The "normal" chemical-mixing energy and the influence of magnetism are distinguished by comparing magnetic and nonmagnetic calculations for similar systems.

DOI: 10.1103/PhysRevB.74.094435 PACS number(s): 75.50.Bb, 75.40.Mg

## I. INTRODUCTION

Fe-Cr alloys are commonly used as structural materials in present fission reactors. Due to their resistance to swelling, low ductile-to-brittle transition temperature, and their low-activation properties, they are also being considered for use in future fusion reactors.[1,2] In both applications the alloys will suffer extensive damage from high-energy particle bombardment. In fusion reactors, 14 MeV neutrons are the main cause of damage. The number of times atoms of some components would be knocked irreversibly from their lattice sites during the lifetime of a fusion reactor would be ~50–150 (Ref. 3). Therefore Fe-Cr alloys would have to be very resilient in recovering from the damage that is inflicted on them during reactor operation. Insufficient damage recovery may lead to component failure due to radiation embrittlement or swelling.

As a prelude to studying the energetics of defect creation and migration that are involved in the evolution of radiation damage, we report here a detailed density functional theory (DFT) study of defect-free Fe-Cr alloys. There are several reasons for initially looking at defect-free FeCr. Firstly is to gain a general understanding of Fe-Cr stability in the absence of vacancies and interstitials. Secondly, Olsson *et al.*[4,5] reported an interesting anomaly in the heat of formation $\Delta E_f$ for FeCr, namely, a small negative $\Delta E_f$ appeared at low Cr concentrations, but $\Delta E_f$ changed sign at higher Cr concentrations; we wished to investigate the reason for this anomalous behavior, emphasizing a real-space description of the Cr-Cr interactions, in contrast to the description in terms of densities of states given by Olsson *et al.*[5] Thirdly, the DFT data can be used as input for parametrizing simpler models that in turn can be used to calculate a phase diagram, or to study the energetics and dynamics of more complex or larger systems.[6] Lastly, by studying defect-free FeCr one can learn what a "typical" or "representative" small piece of FeCr with a particular Cr concentration looks like. Such a structure could then serve as a starting configuration in which to insert interstitials or other defects.

In the present study, the electronic structure and $\Delta E_f$ of 65 Fe-Cr structures have been determined. These structures cover the full Fe-Cr composition range, but the largest number of structures have Fe-rich compositions, as Fe-rich alloys are the most relevant for fusion reactors. Most of these were strongly mixed systems, i.e., Fe had as many Cr nearest neighbors as possible and vice versa. For most compositions several different configurations were calculated, sampling a wide range of different behaviors. All degrees of freedom, including the magnetic moments, were allowed to relax. Apart from providing $\Delta E_f$ data, the DFT calculations have been used to study various other aspects of FeCr, notably the interesting magnetic situation that arises when metals with ferromagnetic and antiferromagnetic properties are mixed. In an attempt to separate the "normal" chemical-bonding energy between Fe and Cr from the magnetic contribution, the magnetically relaxed structures have been recalculated in the non-spin-polarized state. The energetics have also been calculated without self-consistently relaxing the electron density or the ion positions, showing that the main effects are reproduced on a perfect-unrelaxed lattice, without self-consistency.

## II. COMPUTATIONAL DETAILS

The DFT calculations were carried out using VASP.[7,8] VASP is a plane-wave DFT code that implements the projector augmented wave (PAW) method.[9,10] Standard PAW potentials supplied with VASP were used, with exchange and correlation described by the PBE parametrization in the generalized gradient approximation. Fe and Cr potentials with 14 and 12 valence electrons, respectively, were used. The plane-wave energy cutoff was set to 400 eV, which is sufficient for absolute-energy convergence for both Fe and Cr. A 400 eV energy cutoff is also sufficient to avoid energy discontinui-

 

ties in calculations where the cell volume and shape are allowed to relax. Brillouin zone sampling was done using the Monkhorst-Pack scheme. The number of $k$-points was chosen to be sufficient for absolute-energy convergence unless mentioned otherwise. For the nonmagnetic recalculation of the magnetically relaxed structures this sometimes required an increase in the number of $k$-points.

Atomic positions, cell shape, and cell volume of the Fe-Cr configurations were all fully relaxed. The relaxation sometimes resulted in slight shearing of the supercells. For technical reasons, those relaxations that included volume relaxation were usually carried out in two steps. The first step consisted of a relaxation, using Methfessel-Paxton smearing,[11] in which slightly fewer $k$-points were sometimes used. Then the relaxed structure was recalculated with a redefined plane-wave basis set using the tetrahedron method and a sufficient number of $k$-points for absolute-energy convergence.

During the final recalculations of the relaxed structures the numbers of electrons and the magnetic moments within spheres centered on the atomic sites were evaluated. This evaluation requires a sphere radius to be chosen, which was set to 1.4 Å for both Fe and Cr. At this radius, the number of electrons inside the spheres is approximately equal to the total number of electrons inside the supercell (tested for pure unit cells). The 1.4 Å radius is somewhat larger than the standard radius indicated in the VASP Fe and Cr potential files, which may explain in part why the magnetic moments on Cr atoms in this paper are bigger than those reported by some others. For Cr the magnitude of the magnetic moment is especially sensitive to the radius, as the spin density ($\rho_{\text{up}}$-$\rho_{\text{down}}$) is high in the region where the sphere radius is usually chosen. For Fe the choice is less important as the spin density has high values only near the core of the atom.

## III. RESULTS

### A. Pure element reference states

The reference states of the pure elements from which the heats of formation are calculated should be their electronic ground states at their equilibrium volumes. All our calculations are at 0 K. For Fe we find a ferromagnetic (FM) 0 K body-centered-cubic (bcc) lattice spacing of 2.829 Å and a magnetic moment of $2.2\mu_B$. The magnetic moment is in good agreement with experiments, and as expected the 0 K lattice parameter is smaller than the experimental lattice parameter of 2.867 Å.[12] For Cr the situation is less clear. For pure Cr the experimental electronic ground state consists of a spin-density wave with a long wavelength. Cr can also assume a simpler antiferromagnetic (AFM) state in which every atom is surrounded by atoms with moments that are equal in magnitude but opposite in sign to itself (i.e., a bcc lattice with all the atoms at the corners of unit cells having opposite spin to the atom at the center). The energy difference between the spin-density-wave state and the AFM state is small and in the presence of dilute impurities Cr will adopt an AFM structure.[13] Therefore we have taken AFM Cr as the reference state. The equilibrium 0 K lattice parameter in the AFM state is 2.863 Å, again slightly smaller than the experimental value of 2.91 Å,[14] and well within the range of values reported from other electronic-structure calculations.[13] The magnetic moment within 1.4 Å spheres around the Cr nuclei is 1.1, also within the large variation in the magnitude of the Cr moments reported by different authors (0.59 to $1.55\mu_B$).[13] The sensitivity to the sphere radius and the fact that there is such a large range in the literature indicates that while trends in the Cr moments are very useful, the exact magnitudes of the moments may be less meaningful.

The equilibrium unit cells were also recalculated at the same lattice parameter in a nonmagnetic state. For Fe this resulted in a system energy that was 0.546 eV/atom higher than the FM state, in reasonable agreement with results from Jiang *et al.*,[15] who reported a value of 0.56 eV/atom. For Cr the nonmagnetic energy was only 0.014 eV/atom higher than the AFM state. Finally, the Fe unit cell was relaxed to its nonmagnetic bcc equilibrium lattice parameter, which turned out to be 2.756 Å. The energy difference between the magnetic and nonmagnetic Fe unit cells at their respective equilibrium volumes was 0.476 eV/atom, in reasonable agreement with the value of 0.502 eV/atom found by Gonzales-Ormeño *et al.*[16]

### B. Magnetism in FeCr

The magnetic situation that arises when Fe and Cr are mixed is quite interesting. Several different situations can be distinguished, based on the Cr concentration and whether or not the system exhibits magnetic frustration.

Magnetic frustration occurs when it is impossible for some of the Fe and Cr atoms in a configuration to assume a FM or AFM state, respectively, with reference to all their neighbors. Consider a piece of Fe containing two Cr atoms, far apart from each other. The Fe atoms will have their magnetic moments FM aligned. The AFM preference of the Cr atoms will cause them to have their moments AFM aligned to the Fe moments. But what happens if the Cr atoms are moved into nearest-neighbor positions? If both Cr atoms align AFM to the surrounding Fe, they will be FM aligned to each other. Alternatively, the moments on the Cr atoms could be AFM aligned to each other, but then one Cr atom must be FM aligned to the surrounding Fe. Other options can be envisaged, but they all involve AFM alignment of some Fe moments. We will now look in more detail at the different magnetic scenarios that are actually predicted to occur in FeCr.

#### *1. Low Cr concentration, no magnetic frustration*

The magnetic situation in dilute Fe-Cr alloys is straightforward: the Fe atoms have their magnetic moments aligned FM of course, and the single Cr atoms have their moments aligned AFM to the surrounding Fe atoms. The magnitude of the moments on Fe atoms next to a Cr atom hardly changes due to the presence of the Cr atom. Conversely, the AFM moment on the Cr atom surrounded by Fe is significantly larger than the moment on Cr atoms in pure Cr ($1.1\mu_B$ for pure Cr, $\sim 1.8\mu_B$ for a single Cr atom in a $3\times3\times3$ supercell Fe-Cr system).

#### *2. Low Cr concentration, magnetic frustration*

If the Cr concentration is raised beyond very dilute levels, there will occasionally be situations where Cr atoms become

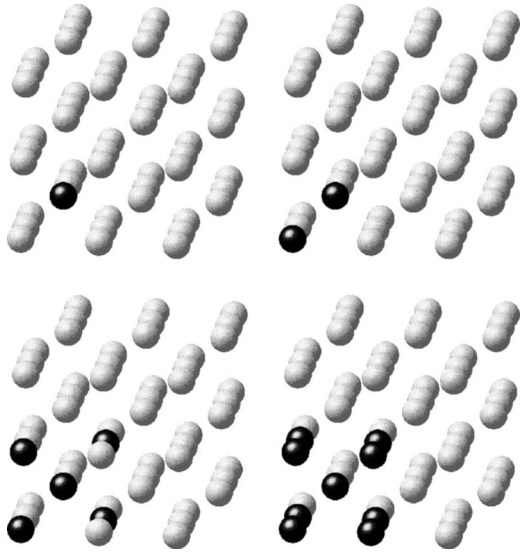

FIG. 1. Systems of $3\times3\times3$ bcc Fe cells with one central Cr atom that has had 0, 1, 4, and all 8 of its nearest-neighbor Fe atoms replaced by Cr.

nearest neighbors, causing magnetic frustration. In order to get a more systematic insight into what happens in magnetically frustrated systems, a series of nine calculations of 3 $\times3\times3$ bcc cells (54 atoms per supercell) has been performed. The first system had just one Cr atom per supercell. In the subsequent systems, the eight nearest-neighbor Fe atoms of the first Cr atom are replaced one by one by other Cr atoms. Figure 1 shows four of the nine systems and Fig. 2(a) shows the evolution of the magnetic moments on the Cr atoms.

Figure 2(a) shows an interesting pattern in the evolution of the magnetic moments. As mentioned before, the single Cr atom has a large AFM moment. Inserting a second Cr atom causes frustration. Out of all the possible scenarios to deal with the frustration, AFM alignment of the two Cr moments to Fe and FM alignment to each other yields the lowest system energy. This is not surprising, as the FM-ordering energy for Fe was calculated to be 0.546 eV/atom while for Cr it was only 0.014 eV/atom (see Sec. III A). It is therefore reasonable to expect that in case of frustration the Cr atoms will be the ones forced into magnetic states that contradict their pure-element tendencies, and this is indeed what was observed in all our calculations. For a nearest-neighbor pair along ⟨111⟩ the magnitude of the moments on the two nearest-neighbor Cr atoms is similar for both atoms, and less than that of a single Cr atom. When a third Cr atom is added along ⟨111⟩ the two outer Cr atoms only have the one central atom to frustrate them; they do not strongly frustrate each other. Therefore their magnetic moments are almost identical

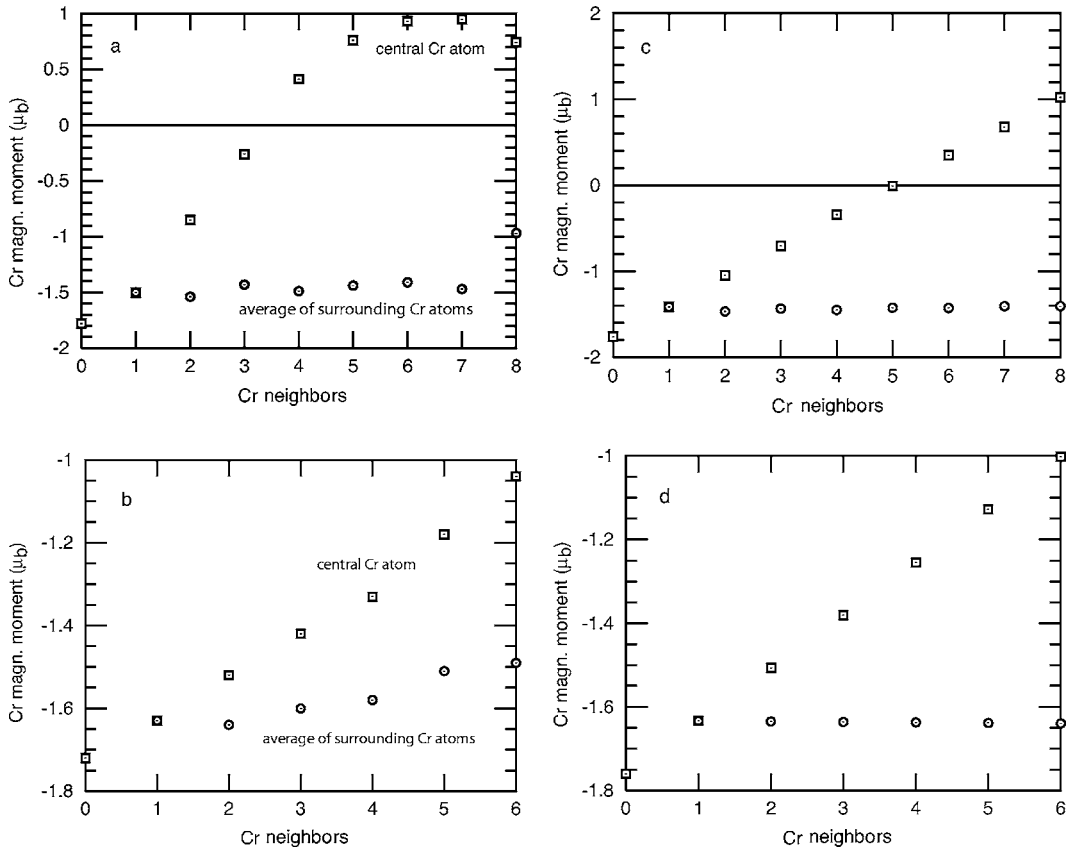


FIG. 2. Evolution of the magnetic moments on Cr atoms in Fe (see also text, Figs. 1 and 3). The squares represent the moment on a central Cr atom as either its nearest-neighbor (a) or next-nearest-neighbor (b) Fe atoms are replaced one by one by Cr atoms. The leftmost data point represents just the single Cr atom in Fe. The circles represent the average of the moments on the Cr atoms that surround the central Cr atom. All the Fe atoms have moments with positive sign. (c) and (d) are the results of the simple model described in the text.

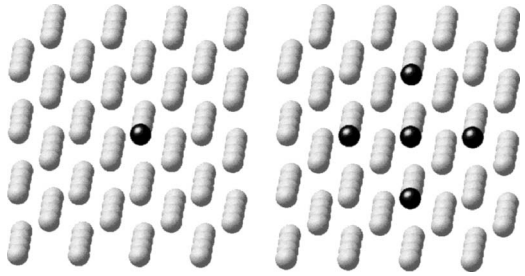

FIG. 3. Systems of $4\times4\times4$ bcc Fe cells with one central Cr atom (left), and the same system in which four of the next-nearest-neighbor Fe atoms of the original Cr atom have been replaced by Cr atoms (right).

to the Cr moments in the system with just two Cr atoms. On the other hand the central Cr atom is now frustrated by two nearest-neighbor Cr atoms, which would prefer the central atom to change the sign of its moment. Two neighboring Cr atoms are still not enough to reverse its moment, but the magnitude of the moment on the central Cr atom is reduced further. This pattern continues as more Fe atoms are replaced by Cr. When going from four to five Cr neighbors, the moment on the central atom changes sign and assumes a slightly AFM alignment with respect to the outer Cr atoms. When the number of Cr neighbors is increased further, the influence of the Fe atoms disappears completely, and with it, the nearest-neighbor magnetic frustration. When the central Cr atom is surrounded by eight Cr nearest neighbors its moment is parallel to the Fe moments and AFM to all the nearest-neighbor Cr atoms. While most of Fig. 2(a) fits the pattern described above very well, the last data point seems out of place. It seems strange that introducing one more Cr atom would decrease the magnitude of the moments on all the outer Cr atoms by more than a third. In the system with nine Cr atoms the moments on the Fe atoms are very similar to the Fe moments in systems with fewer Cr atoms (a variation around the bulk value of a few tenths of a $\mu_B$ at most for systems with seven or eight Cr atoms, a variation of just a few hundredths of a $\mu_B$ for the system with a single Cr atom).

A confirmation that magnetic frustration is indeed the cause of the change in sign in Fig. 2(a) was obtained from a series of calculations in which not the nearest, but the next-nearest-neighbor Fe atoms around a central Cr atom were successively replaced by Cr atoms (see Fig. 3). These calculations were carried out in a larger supercell comprising $4\times4\times4$ bcc cells. $k$-point convergence for these calculations was not absolute and a different smearing method was used. Therefore these structures are not included in the $\Delta E_f$ data. The results are shown in Fig. 2(b). As expected, in contrast to Fig. 2(a), Fig. 2(b) shows no change in sign of the moment on the central Cr atom although its magnitude changes as its next-nearest Fe neighbors are replaced by Cr atoms.

The general behavior described above in words can be captured by a simple phenomenological model of the Heisenberg type, in which for the nearest-neighbor cluster of $n+1$ atoms we write the magnetic energy as

$$U = nJ_1xy + J_2(8-n)x + 7J_2ny + J_3n_{2\mathrm{Cr}}y^2 + 6J_4x + (n_{2\mathrm{Fe}}-6)J_4y + x^2 + ny^2. \quad (1)$$

$x$ and $y$ are the moments of the central Cr atom and of the surrounding Cr neighbors, respectively, in units of the Fe moment. We assume for simplicity that these neighbors have identical moments and that the iron moments remain constant, which approximate the results of our calculations. The parameters $J_1$, $J_2$, $J_3$, and $J_4$ couple the Cr-Cr first-neighbor moments, Cr-Fe first-neighbor moments, the Cr-Cr second-neighbor moments, and the Cr-Fe second-neighbor moments, respectively. $n_{2\mathrm{Cr}}$ and $n_{2\mathrm{Fe}}$ are the numbers of second-neighbor Cr-Cr and Cr-Fe bonds. The final squared terms are the self-energies that inhibit spontaneous polarization, and these define the unit of energy, which is arbitrary for present purposes. A similar model can be written down in a straightforward way for the case of the next-nearest-neighbor Cr clusters, without a term for coupling nearest-neighbor Cr-Cr moments

$$U = nJ_3xy + 8J_2x + 8nJ_2y + (6-n)J_4x + 5nJ_4y + x^2 + ny^2. \quad (2)$$

The following parameters gave the results shown in Figs. 2(c) and 2(d):

$$J_1 = 0.3, \quad J_2 = 0.125, \quad J_3 = 0.02, \quad J_4 = 0.1.$$

.

These parameters were not fitted algorithmically to the database of moments, but chosen by trial and error to illustrate the trends. We see that this model reproduces some of the qualitative features of the DFT calculations, particularly in the case of second neighbors, namely, that the central Cr moment varies rapidly with the number of Cr neighbors in order to align antiferromagnetically with them, while the Cr atoms on the outside of the cluster change their moments much less. However, for the nearest-neighbor shell [comparing Figs. 2(a) and 2(c)] it does not capture the negative curvature as the shell of nearest neighbors becomes full, in particular, the anomalous behavior as the last atom is added. These effects may be related to our approximation of constant moments on the Fe. The appearance of degenerate states in the cubic-point symmetry that is achieved when the Cr nearest-neighbor shell is complete might also affect the final point.

#### *3. High Cr concentration*

The pattern of magnetic ordering described in Sec. III B 2 can be extended to higher Cr concentrations. As long as the Fe atoms still have some Fe as nearest neighbors, the outcome is always that the moments on the Fe atoms are FM aligned, with moments close in magnitude to bulk Fe. The moments on the Cr atoms are then arranged in a fairly predictable way that avoids magnetic frustration as much as possible. As long as the initial spins on the Fe atoms are aligned in parallel, the self-consistent moments always converge to the same solution for Fe-rich FeCr without much difficulty, regardless of the initial spins on the Cr atoms. As the Cr concentration is increased further, at some point the number of metastable solutions that can appear starts to increase. The lowest-energy solution is generally one in which the Fe atoms have large moments, but if Fe atoms have only Cr neighbors, the signs of the Fe moments that lead to the

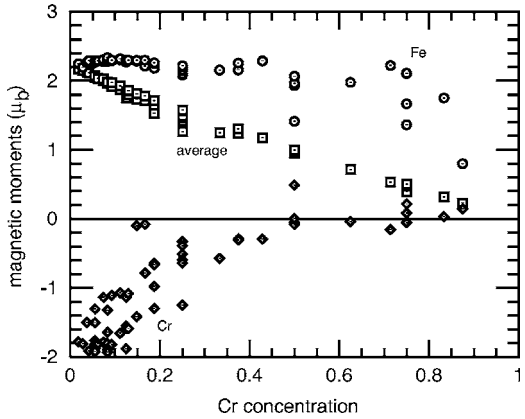


FIG. 4. The magnitude of magnetic moments on atoms in FeCr as a function of concentration. The circles, diamonds, and squares indicate the moments on Fe atoms, Cr atoms, and the average, respectively. The large variation in the magnitude of the Cr moments appears because systems with both clustered and monatomically dispersed Cr atoms are represented. In the dispersed systems all Cr atoms have large negative moments; in the clustered configurations the moments are on average less negative due to frustration.

lowest energy are unpredictable. For the moments on the Cr atoms the situation is even less predictable, as they not only have unpredictable signs but can also vary in magnitude from zero to values larger than the pure Cr bulk moments. Therefore, finding what can reasonably be assumed to be the lowest-energy solution requires starting from a number of configurations with different initial moments.

Figure 4 shows the magnitude of the magnetic moments in FeCr as a function of concentration. The large variation in the magnitude of the Cr moments appears because systems with both clustered and monatomically dispersed Cr atoms are represented. In the dispersed systems all Cr atoms have large negative moments; in the clustered configurations the moments are on average less negative due to frustration. Figure 4 is in good agreement with tight binding-linearized muffin-tin orbitals calculations by Mirzoev *et al.*[17] and the average-moment data are in good agreement with bulk-magnetization-force measurements by Aldred.[18] Kajzar and Parette[19] did diffuse neutron-scattering experiments on FeCr with very low Cr concentrations. For 1.46 at. % Cr they found an AFM moment on the Cr atoms of $-1.88\mu_B$, which is in good agreement with our results. Figure 4 shows the trends described in Sec. III B 1, III B 2, and III B 3 quite clearly: the moments on the Fe atoms remain approximately constant up to high Cr concentrations and in Fe-rich FeCr the Cr atoms have large AFM moments. As the Cr concentration increases, the moments on the Cr atoms are reduced due to frustration. As the Cr concentration increases further, the structures draw closer to AFM Cr, giving a net magnetic moment on the Cr atoms that draws closer and closer to zero. As a result, the average moment decreases roughly linearly from the bulk Fe value for pure Fe to zero for pure Cr.

### C. Heats of formation and pair interactions

The heat of formation per atom $\Delta E_f$ of 65 FeCr structures has been determined by relaxing all degrees of freedom for

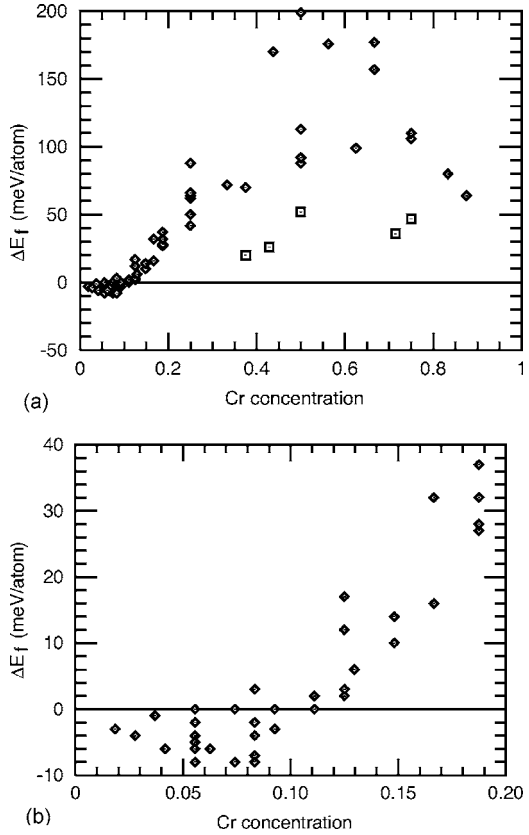


FIG. 5. (a) The 0 K heat of formation $\Delta E_f$ of Fe-Cr structures in their magnetic ground state. The five data points with squares indicate systems that were not very well mixed, i.e., Fe interacted mostly with Fe and Cr mostly with Cr, which explains the low $\Delta E_f$ values. (b) A close-up of the Fe-rich part of the concentration range.

these structures. For a system of $n$ atoms and composition $Fe_xCr_{1-x}$, $\Delta E_f$ is calculated according to

$$\Delta E_f = \frac{E(\mathrm{Fe}_x\mathrm{Cr}_{1-x}) - xnE_{\mathrm{ref}}(\mathrm{Fe}) - (1-x)nE_{\mathrm{ref}}(\mathrm{Cr})}{n}, \quad (3)$$

where $E_{\mathrm{ref}}$(Fe) and $E_{\mathrm{ref}}$(Cr) are the energies per atom of Fe and Cr in their pure equilibrium states. For a few systems the relaxation was split into two parts, i.e., the ionic relaxation was carried out separately from the volume and shape relaxation before the final recalculation with a new basis set (see Sec. II). These few tests showed that the main contribution of the relaxation energy comes from ionic relaxation. The structures varied in size from the two-atom $B2$ structure to 15 systems of $3\times3\times3$ bcc cells with 1–9 Cr atoms and one system of $4\times4\times4$ bcc cells with 64 Cr and 64 Fe atoms. The reference states for Fe and Cr consisted of the pure-element unit cells at their equilibrium spacing. For some of the larger FeCr systems the reference state for Fe consisted of a large pure-Fe system, e.g., in the $2\times2\times3$ cells Fe23-Cr1 system, the reference state is taken as $(23/24)*E(\mathrm{Fe24})+E(\mathrm{Cr1})$. This reduces the nonsystematic error by comparing systems of similar size. The resulting $\Delta E_f$ for the Fe-Cr structures is shown in Fig. 5. Our results show a mostly positive $\Delta E_f$ of up to ~100 meV/atom with a

small negative $\Delta E_f$ down to −8 meV/atom at the Fe-rich end. These results agree with calculations by Olsson *et al.*[4,5] and Mirzoev *et al.*[17] It should be noted that at any particular concentration $\Delta E_f$ can vary considerably, depending on the arrangement of the atoms. In particular, where $\Delta E_f$ is positive a complete phase separation would have the lowest energy, at least if the supercell were sufficiently large. Therefore at the Cr-rich end of the concentration range there are very probably structures with lower $\Delta E_f$ than those in Fig. 5, even in the supercells we have used. Since most of the data points in the Cr-rich end of the concentration range were strongly mixed systems, i.e., Fe had as many Cr nearest neighbors as possible and vice versa, these data points are probably at or near the maximum of $\Delta E_f$, and they probably do not include the minimum. Moreover, Olsson[4] showed that for structures with a substantial amount of Cr the paramagnetic phase has a lower $\Delta E_f$ than the ferromagnetic phase. At the Fe-rich end of the concentration range the situation is different. Many Fe-rich structures have been calculated, representing many different coordinations, and the negative $\Delta E_f$ region has been well sampled. It is therefore unlikely that structures with a substantially lower $\Delta E_f$ will be found.

The mostly positive $\Delta E_f$ is in agreement with the absence of any intermetallic phases at low temperature in the Fe-Cr phase diagram (see Fig. 6).[20] The small negative $\Delta E_f$ for some Fe-rich structures could theoretically give rise to some ordered compounds, but the minimum $\Delta E_f$ is only −8 meV/atom, about 10% of the average atomic-vibration energy at room temperature. Therefore the absence of such an ordered phase in the phase diagram does not contradict our $\Delta E_f$ data. There is still a discrepancy between our data and the Cr solubility limit at low temperature in the published-phase diagram. If one were to draw the tie line between the lowest-energy data points in Fig. 6 and the (defined, not shown) $\Delta E_f$=0 data point for pure Cr, the resulting solubility limit is ~8% at low temperature. At higher temperature, the solubility should increase to higher values. However, according to the published-phase diagram, the Cr solubility limit at 500 K would be only ~2%. It should be noted that at low temperatures the time required for Fe-Cr alloys to reach thermodynamic equilibrium becomes excessively long. The lowest-temperature-relevant experimental data for FeCr that we are aware of were measured at just under 700 K.[21] The solubility line at low temperature is therefore an extrapolation over several hundred Kelvin, made without knowledge of the negative $\Delta E_f$ for low Cr concentrations. Moreover, Sagaradze *et al.*[22] found that Fe-Cr alloys with 5 and 9 wt. % Cr do indeed show ordering after thermal annealing and electron irradiation, while alloys with Cr concentrations of 13% or higher show the formation of a Cr-rich phase. Their results are not necessarily inconsistent with the published-phase diagram because their samples contained small traces of other elements, but they do provide some confirmation of our results.

It is of interest to explore why the negative $\Delta E_f$ at low Cr concentrations, which is associated with a negative heat of solution of single Cr atoms, becomes positive in the range 10–12 %. Olsson *et al.*[4,5] considered this in terms of the total electronic density of states. They observed that an occupied peak just below the Fermi energy in the minority band of

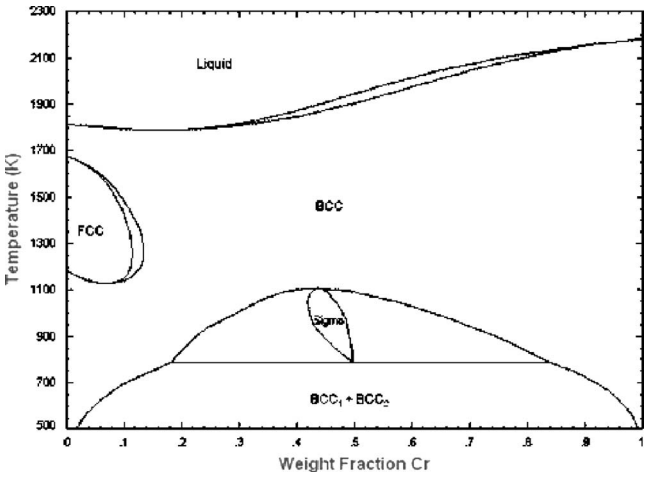


FIG. 6. The Fe-Cr phase diagram (Ref. 20). Note that the phase diagram has the weight fraction on the horizontal axis, whereas other figures in this paper use the atomic fraction. Since Fe and Cr have rather similar mass, the differences between the two approaches are small.

pure Fe moved to lower energy and became depleted with the addition of Cr. This would be associated with a decrease in the band-energy contribution to the total energy. At higher concentrations this peak continues to empty, but by a process of moving back to higher energy and squeezing under the Fermi level as it does so. This behavior would be expected to increase the band energy again. In our real-space picture, the simplest explanation is a repulsive pairwise Cr-Cr interaction. Figure 7 shows DFT results for $\Delta E_f$ of systems of various sizes with two Cr atoms at different separations. The first conclusion that can be drawn from Fig. 7 is that even when going from $2\times2\times3$ to $3\times3\times3$ supercells, the system size is not yet converged as far as $\Delta E_f$ of nearest-neighbor Cr pairs is concerned. The proximity of periodic images of Cr atoms in neighboring supercells also appears to be the cause of the rise in $\Delta E_f$ at the fifth-neighbor separation (Cr atoms

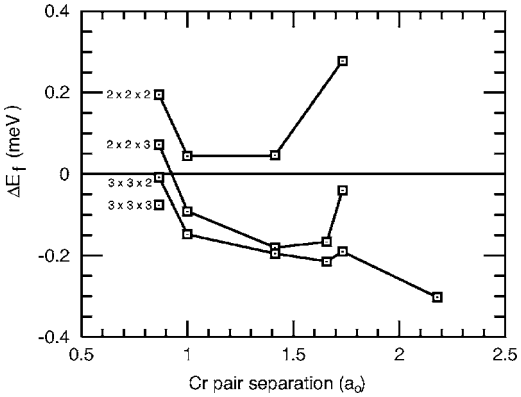


FIG. 7. The heat of formation of systems of various sizes, containing two Cr atoms at different separations. The number of unit cells of the systems is indicated next to the data points. Note that since systems of different sizes are being compared, $\Delta E_f$ is indicated as an absolute value, not in meV/atom. For $3\times3\times3$ unit-cell systems there is only one data point, i.e., the energy for the situation where the Cr atoms are nearest neighbors.

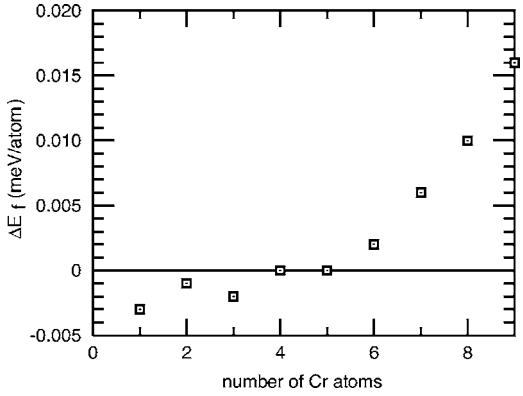


FIG. 8. Heat of formation of $3\times3\times3$ bcc cell Fe systems with Cr clusters ranging from one to nine atoms (see also text; Fig. 1).

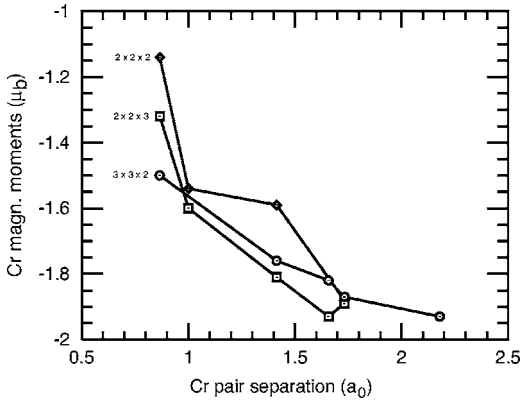


FIG. 9. Magnetic moments on Cr atoms in systems of various sizes containing two Cr atoms. The number of unit cells of the systems is indicated next to the data points. Note that the data point for the second-nearest-neighbor pair in the $3\times3\times2$ cell system is missing.

at a distance of one bcc cell-body diagonal, or 1.73 lattice spacings), as this effect becomes smaller for larger systems. If we ignore this effect, the conclusion is that for all system sizes the system with two Cr atoms as nearest neighbors has the highest energy and the system energy decreases monotonically with separation for an isolated pair by at least 0.3 eV. Such a tendency to maximize Cr-Cr separations would favor ordering. This is in agreement with experiments by Mirebeau *et al.* and Sagaradze *et al.*[21,22] which showed ordering at low Cr concentrations, although the experiments did not indicate if this ordering consists of single Cr atoms at maximum separations or something more complicated.

Based on the previous results, a typical starting structure for inserting interstitials into a piece of FeCr with 0–8 % Cr (which will be the topic of future work) would consist of single Cr atoms in solution avoiding nearest neighbors. For the higher part of the 0–8 % concentration range avoiding fifth-neighbor separations between Cr atoms may also be important, and may indeed override the tendency to maximize the distances separating Cr atoms. This will be explored by statistical simulations in a subsequent paper. Section III D below describes some further results, which are relevant to the atomic structure of alloys with Cr percentages $>8\%$.

Finally, in this section we will discuss the importance of different contributions to $\Delta E_f$ for FeCr with higher Cr percentages. It may be tempting to simply extrapolate the picture of lower Cr percentages: Cr atoms repel each other quite strongly, especially at nearest neighbors due to the magnetic frustration, so inserting more and more Cr atoms should eventually lead to a positive $\Delta E_f$. This picture is, however, too simple and our calculations provide quantitative evidence for the multiatom interactions. Nearest-neighbor frustration of the magnetic moments on Cr atoms alone certainly cannot explain the positive $\Delta E_f$ at higher Cr percentages. In the $B2$ structure of $Fe_{0.5}Cr_{0.5}$ there is no nearest-neighbor magnetic frustration. Yet already at $\sim11\%$ Cr $\Delta E_f$ becomes positive. To make the point even clearer, Fig. 8 shows $\Delta E_f$ corresponding to the series of clusters for which the magnetic moments were calculated in Sec. III A 2 (see also Fig. 1). In the systems with 3–5 Cr atoms, the central Cr atom has a very mixed coordination, leading to strong frustration. Nevertheless, $\Delta E_f$ for these systems is lower than for the systems with 7–9 Cr atoms where there is less frustration. Yet another confirmation of the limited relationship between the magnetic moments on the Cr atoms and system energy can be obtained by looking at the magnetic moments of the Cr atoms of the structures represented in Fig. 7. For all three sets of data in Fig. 7 the pattern of the magnetic moments on the Cr atoms is similar: for nearest-neighbor Cr-pair atoms, the moment is smaller in magnitude than the moment on a single Cr atom in a system of similar size, and as the separation between the Cr atoms is increased, the magnitude of the Cr moments draws closer to the value of a single Cr atom in Fe (see Fig. 9). Yet $\Delta E_f$ patterns are not similar, the $2\times2\times2$ and $2\times2\times3$ supercells showing a significant increase in system energy at the fifth-nearest-neighbor separation, while for the $3\times3\times2$ supercell there is hardly any increase. Systems in which the magnetic moments on the Cr atoms are broadly similar can have significantly different energies. One may therefore wonder if magnetic frustration of the Cr moments plays any significant role at all. The answer to this question is given in Fig. 10, which again shows $\Delta E_f$ for Fe-rich structures, but now divided into two categories of data points: those that represent structures without nearest-neighbor frustration and those with frustration. It is clear that

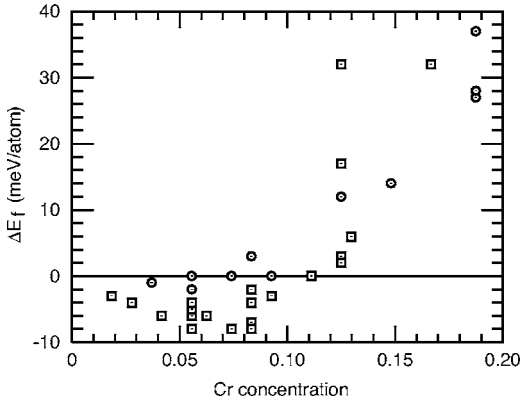


FIG. 10. The FeCr $\Delta E_f$ for Fe-rich structures, categorized into systems with (circles) and without (squares) nearest-neighbor frustration between Cr atoms.

all the 16 systems (some of which are indistinguishable on the graph due to overlapping data points) with the lowest $\Delta E_f$ are those that do not suffer from magnetic frustration. Only two magnetically frustrated systems have a slightly negative $\Delta E_f$, which is within the margin of precision of the DFT calculations. Magnetic frustration therefore has a limited, but still apparent energetic impact, as it correlates almost perfectly with the presence of a negative $\Delta E_f$ in Fe-rich structures. By far the largest and most important effect of magnetic frustration on the energetics within the Fe-Cr system is in the repulsive nearest-neighbor interaction of a Cr-Cr pair, discussed in detail in Sec. III E below.

Seeing that magnetic frustration cannot explain the strongly positive $\Delta E_f$ at higher Cr percentages, one might guess that the latter stems from the long-range pair repulsion between Cr atoms in Fe. As the repulsion reaches at least up to the sixth-neighbor distance, there will be many such repulsive pair interactions even at low Cr percentages. However, Fig. 7 shows that for the $3\times3\times2$ supercell the interaction between Cr pairs, while repulsive, still leads to a negative $\Delta E_f$ at any separation. The superposition of many such interactions could still not explain a positive $\Delta E_f$. Figure 7 also provides a clue to the cause of the positive $\Delta E_f$. In the $3\times3\times2$ supercell the interaction energy between a pair of Cr atoms is negative at any separation. As the system size is reduced, the pair of Cr atoms interacts with the Cr atoms of its own periodic images. But instead of this leading to multiple negative-energy contributions, the resulting energy turns positive. This proves that many-body interactions between the Cr atoms are important. An alternative, equally valid viewpoint within the real-space picture, is that the interactions are concentration dependent. The positive $\Delta E_f$ at higher Cr concentration cannot be explained by the pair interactions alone, which give a reasonable explanation of the behavior of dilute Fe-Cr alloys. It is possible that the many-body interaction can be described, for example, by a concentration-dependent one- and two-body interaction energy, but the best way to represent it is a matter for further research.

### D. Formation energy of small Cr clusters

While the structure of FeCr with low percentages of Cr seems straightforward to understand with the repulsive pair potential, it is unclear what the structure of FeCr with >8% Cr should be. From Fig. 6, in low-temperature equilibrium it should be phase-separated into a dilute solution of Cr in Fe and a Cr-rich phase. In reality this thermodynamic equilibrium will not be reached of course, and a commercial material represents some compromise between the as-cast or possibly heat-treated structure (which may be close to random ordering of the atoms) and fully separated Fe-rich and Cr-rich phases. Calculations to determine how far the structure should have progressed towards equilibrium would involve lengths and time scales many orders of magnitude beyond the scope of DFT, and Monte Carlo calculations or other methods would be far more suitable for that purpose. DFT calculations can nevertheless provide some small-scale information, which may be useful as input to other modeling approaches in which the energies of small clusters are required.

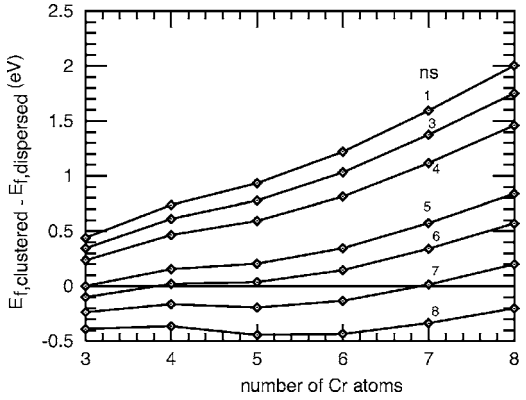


FIG. 11. Energy difference between $3\times3\times3$ bcc cell Fe-Cr systems with Cr atoms in clustered or monatomically dispersed positions. The clustering energy is shown for clusters of different size (number of Cr atoms shown along the horizontal axis) and for different concentrations of monatomically dispersed Cr atoms from which the cluster is created. The concentration *ns* refers to the number of solute Cr atoms in a $3\times3\times3$ bcc cell Fe-Cr system [see also Eq. (4) and text]. So for instance, the data point on the right vertical axis of the curve labeled "4" refers to the formation energy of a cluster of eight atoms created by clustering together atoms from a monatomic solution of 4 Cr atoms per 54 atom Fe-Cr supercell.

With DFT we can obtain the energy difference between systems with Cr atoms dispersed in solution and systems with equal numbers of Cr atoms arranged in small clusters. Systems of $3\times3\times3$ bcc cells with 3–8 monatomically dispersed Cr atoms (the system with eight Cr atoms had one Cr nearest-neighbor pair in it) were fully relaxed; systems of similar size with small Cr clusters were also studied; the results for their magnetic moments were reported in Sec. III B 2. The resulting cluster-formation energy is shown in Fig. 11, which was generated from the equation

$$\Delta E_{\text{cluster}} = E_{f,\text{clustered}} - E_{f,\text{dispersed}}$$

$$= E_{f,\text{cluster}}(\text{Fe}_{\text{N-}nc}\text{Cr}_{nc}) - \frac{nc}{ns}E_f(\text{Fe}_{\text{N-}ns}\text{Cr}_{ns}). \quad (4)$$

In Eq. (4), the first term on the right-hand side is the formation energy of a system of N sites (54 in this case) containing a cluster of *nc* Cr atoms. The second term of the second line on the right-hand side is the formation energy of a system of N sites over which are dispersed in solution *ns* Cr atoms. The prefactor normalizes this to the number of Cr atoms in the cluster.

The trend shown in Fig. 11 is clear: in a dilute solution there is no tendency to favor clustering; this is illustrated by the uppermost curve in Fig. 11, which shows the energy required to assemble a cluster in a dilute solution as a function of the number of clustered atoms. In the limit of large clusters, the slope of the uppermost curve would tend to the heat of solution 0.18 eV per Cr atom. Figure 11 also illustrates the energy for the assembly of small clusters from progressively more concentrated and supersaturated solutions. As the solution becomes supersaturated, going down the sequence of curves in Fig. 11, we see that it becomes

favorable to form a small cluster before a larger one. The monatomic Cr solutions corresponding to the two lowest curves have a positive heat of formation, so these curves must both have asymptotically negative slopes in the limit of large-cluster size. Hence at least the lowest curve, and perhaps also the second lowest, starts with a slightly negative energy and becomes positive over a range of cluster sizes, before becoming negative again in the large-cluster limit. This is different from the behavior of such a curve as drawn in the textbook description of nucleation theory, in which the initial negative energy for very small clusters would be absent. It is not surprising that the concept of interfacial energy breaks down for such small clusters. One is nevertheless inclined to think there is still an "effective" interfacial energy, dependent on cluster size, which one still does not expect to be negative, as it is here.

In interpreting these results we face the difficulty of scatter in the calculated data points, particularly for the supersaturated configurations. For systems with one particular number of Cr atoms only one configuration with clustered Cr atoms and one configuration with dispersed Cr atoms has been calculated. There are many ways to do both, and other choices of clustered or dispersed configurations will result in other energy differences. The statistical basis could be broadened by simply determining the clustered-dispersed energy difference for a larger number of clustered and dispersed configurations, but again this is a task better suited to a statistical simulation, which may be possible using cluster energies fitted with the help of our database.

### E. Nonmagnetic calculations

Given the important role that magnetism has on $\Delta E_f$ in FeCr it may be of interest to try to isolate which part of $\Delta E_f$ is due to magnetism and which part would be contributed by nonmagnetic chemical bonding. At first glance it may seem that the way to achieve this would be to do a nonmagnetic relaxation of the Fe-Cr structures. Unfortunately, this apparently straightforward method is unworkable because nonmagnetic bcc Fe is mechanically unstable ($C'$ is negative), and it would transform to hcp. Therefore we have not carried out nonmagnetic relaxations, but have recalculated the nonmagnetic energy for most of the magnetically relaxed structures reported above. For the reference energies the nonmagnetic energies of pure Fe and Cr at their magnetic-equilibrium lattice parameters were used.

It quickly becomes clear that there is actually no unambiguous answer to the question of how much of $\Delta E_f$ is contributed by magnetism. Atoms with a magnetic moment are slightly larger than nonmagnetic atoms (Ref. 23—as the Fe calculations reported here also exhibit). The nonmagnetic state of a system that was relaxed with magnetism "turned on" will therefore represent a system under positive-volume strain. In the case of Fe-rich structures the stress associated with this strain can be up to 20 GPa, for Cr-rich structures it is ~4 GPa. A system under 20 GPa of tensile stress contains a considerable strain energy. As an example, relaxing only the volume of a $2\times2\times2$ supercell with one Cr atom decreases the energy by 61 meV/atom, which is far more than

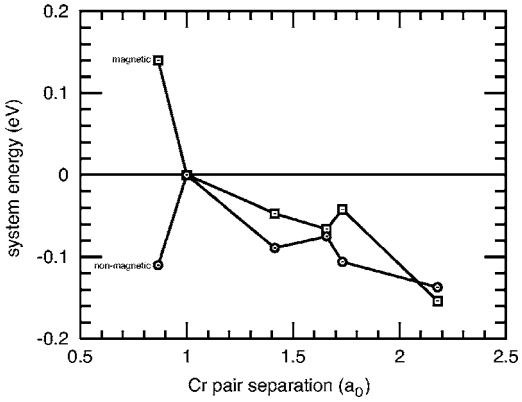


FIG. 12. Magnetic and nonmagnetic energies of $3\times3\times2$ cell systems with two Cr atoms at different separations. The energies have been shifted so that for both cases the energies of the systems with second-nearest-neighbor separation are zero.

the nonmagnetic $\Delta E_f$ of any Fe-Cr structure in our dataset. Therefore the approach of simply switching off magnetism in magnetically relaxed systems does not separate a nonmagnetic effect from the effect of strain energy.

While the inability to isolate the nonmagnetic energy in this way is disappointing, some interesting data can be extracted from the nonmagnetic calculations. One result concerns the long-range repulsion between Cr atoms. Figure 7 showed a decrease in the system energy as the Cr pair separation in $3\times3\times2$ cell systems was increased. This can be compared to the values found for the equivalent nonmagnetic structures because all $3\times3\times2$ cell nonmagnetic systems with two Cr atoms are under approximately the same stress and thus contain a roughly equal amount of strain energy. The minimum and maximum of the stresses averaged over the three Cartesian directions are only 0.5 GPa apart. Figure 12 shows the energies of magnetic and nonmagnetic $3\times3\times2$ supercells with two Cr atoms. The energy axis has been shifted to make the energies of systems with second-nearest-neighbor Cr separation equal to zero for both cases. Figure 12 shows that the nearest-neighbor repulsion in magnetic FeCr is indeed due to magnetism, as it has completely changed sign in the nonmagnetic Fe-Cr case shown in Fig. 12. The long-range repulsions for the magnetic and nonmagnetic cases are rather similar to each other: on increasing the Cr separation from second-nearest neighbor to sixth-nearest neighbor, the system energy decreases almost monotonically by ~0.15 eV in both cases. Since the long-range repulsion is apparently not magnetic in nature, there must be some other explanation for it. Elastic effects are long ranged, but it seems unlikely that that explains the results in FeCr where the two atoms are so similar in size, and we have indeed ruled this out by reproducing the effect without any relaxation of atomic positions. Lattice relaxation in these cases changes the total energies by less than 0.01 eV, except when the two Cr atoms are nearest neighbors. We have also considered the sum of one-electron eigenvalues in an attempt to isolate the nature of the electronic repulsion. This sum increases with separation, that is, it provides an attractive contribution to the energy. Thus there appears to be no simple explanation in terms of electronic structure for the origin of

the long-range repulsion between Cr atoms in Fe.

Finally, the forces acting on atoms in the nonmagnetic structures were investigated. In nonmagnetic FeCr the atoms will generally have equilibrium positions, which are slightly different from the magnetically relaxed situation, not just because of the smaller overall volume but also in terms of relative distances between atoms. We checked whether switching off magnetism would systematically increase or decrease the distance between Cr atoms and the surrounding Fe atoms in Fe-rich structures. This turned out not to be the case. While forces up to a few tenths of an eV/Å were present in the nonmagnetic structures, there was no simple pattern to them that suggested a systematic relative increase or decrease in the Fe-Cr bond lengths.

## IV. SUMMARY AND CONCLUSIONS

DFT calculations on 65 fully relaxed Fe-Cr structures have confirmed in more detail the $\Delta E_f$ anomaly in FeCr first reported by Olsson *et al.*[4,5] and Mirzoev *et al.*[17] While $\Delta E_f$ is positive for most concentrations, in accordance with the large immiscibility gap in the experimental-phase diagram, a small negative $\Delta E_f$ with a minimum of $-8$ meV/atom is found for Cr concentrations below 12 at. %. These results indicate that the low-temperature Cr solubility in the experimental-phase diagram, which has been extrapolated from high-temperature measurements, probably underestimates the actual value that should exceed 8 at. % based on our calculations.

We have explained the observed results in terms of a real-space description of the Cr-Cr interactions. The origin of the negative $\Delta E_f$ lies in the negative heat of solution of single-Cr atoms, which quickly disappears as the concentration is increased because Cr atoms in Fe repel each other. The repulsion between Cr atoms is significant at least up to the sixth-neighbor distance and is quite strong for nearest neighbors. The strong nearest-neighbor repulsion is caused by magnetic frustration. Magnetism therefore inhibits segregation of Cr-rich phases. The long-range repulsion is electronic in origin, as we conclude from our finding that lattice relaxation changes the energy by less than 0.01 eV. However, it is not a specifically magnetic effect, since a nonmagnetic calculation at fixed atomic positions reproduces the repulsion. Nor is it reproduced simply by the eigenvalue sum.

The positive $\Delta E_f$ at higher Cr percentages is caused by many-body interactions, or concentration-dependent interactions, not by the nearest-neighbor magnetic frustration. This is demonstrated by building structures with Cr clusters having no magnetic frustration, yet still having a positive $\Delta E_f$ compared to the pure phases.

The behavior of the clustering energy in a supersaturated solution is anomalous in comparison to what one might expect from the textbook description of nucleation theory. Namely, we find the smallest clusters are stable compared to the dispersed atoms, whereas those of intermediate size are unstable with respect to dispersed atoms.

The magnetic moments of nearest-neighbor clusters of 1–9 atoms and second-neighbor clusters of 1–7 atoms were studied, showing how the magnetic frustration on the central Cr and surrounding Cr atoms is altered according to the number of antiferromagnetic Cr neighbors. A simple Heisenberg-type model explained the qualitative effects, but could not account for the saturation and final decrease of the moment of the central atom as the number of Cr in its nearest-neighbor shell went from seven to eight. We suspect these effects to be related to details of the electronic structure, such as the increase in degeneracy that results when the cube of neighbors is completed.

The data we have generated are being used as input for statistical-thermodynamic studies of the structures, and we hope they will prove useful in the future as input for benchmarking semiempirical models of the interatomic forces.

## ACKNOWLEDGMENTS

The authors wish to thank David Pettifor and Sergei Dudarev for helpful discussions. We are grateful to the EPSRC for support under Grant No. GR/S88352/01.

*Electronic address: t.p.c.klaver@qub.ac.uk
†Present address: Department of Materials, Imperial College London, Exhibition Road, London SW7 2AZ, United Kingdom.

[1] A. Hishinuma, A. Kohyama, R. L. Klueh, D. S. Gelles, W. Dietz, and K. Ehrlich, J. Nucl. Mater. **258-263**, 193 (1998).
[2] F. A. Garner, M. B. Toloczko, and B. H. Sencer, J. Nucl. Mater. **276**, 123 (2000).
[3] S. J. Zinkle, Phys. Plasmas **12**, 058101-8 (2005).
[4] P. Olsson, I. A. Abrikosov, L. Vitos, and J. Wallenius, J. Nucl. Mater. **321**, 84 (2003).
[5] P. Olsson, I. A. Abrikosov, and J. Wallenius, Phys. Rev. B **73**, 104416 (2006).
[6] D. Farkas, C. Schon, M. S. F. Lima, and H. Goldenstein, Acta Mater. **44**, 409 (1996).
[7] G. Kresse and J. Hafner, Phys. Rev. B **47**, RC558 (1993).
[8] G. Kresse and J. Furthmuller, Phys. Rev. B **54**, 11169 (1996).
[9] P. E. Blöchl, Phys. Rev. B **50**, 17953 (1994).
[10] G. Kresse and D. Joubert, Phys. Rev. B **59**, 1758 (1999).
[11] M. Methfessel and A. T. Paxton, Phys. Rev. B **40**, 3616 (1989).
[12] R. Kohlhaas, P. Donner, and N. Schmitz-Pranghe, Z. Angew. Phys. **23**, 245 (1967).
[13] R. Hafner, D. Spišák, R. Lorenz, and J. Hafner, J. Phys.: Condens. Matter **13**, L239 (2001).
[14] R. G. Ross and W. Hume-Rothery, J. Less-Common Met. **5**, 259 (1963).
[15] C. Jiang, C. Wolverton, J. Sofo, L. Chen, and Z. Liu, Phys. Rev. B **69**, 214202 (2004).
[16] P. G. Gonzales-Ormeño, H. M. Petrilli, and C. G. Schön, CALPHAD: Comput. Coupling Phase Diagrams Thermochem. **26**, 573 (2002).
[17] A. A. Mirzoev, M. M. Yalalov, and D. A. Mirzaev, Phys. Met. Metallogr. **97**, 336 (2004).

[18] A. T. Aldred, Phys. Rev. B **14**, 219 (1976).
[19] F. Kajzar and G. Parette, Phys. Rev. B **22**, 5471 (1980).
[20] www.factsage.com
[21] I. Mirebeau, M. Hennion, and G. Parette, Phys. Rev. Lett. **53**, 687 (1984).
[22] V. V. Sagaradze, I. I. Kositsyna, V. L. Arbuzov, V. A. Shabashov, and Y. I. Filippov, Phys. Met. Metallogr. **92**, 505 (2001).
[23] E. W. Lee, Rep. Prog. Phys. **18**, 184 (1955).